2023 IEEE XVI International Scientific and Technical Conference Actual Problems of Electronic Instrument Engineering (APEIE) | 979-8-3503-3088-5/23/$31.00 ©2023 IEEE | DOI: 10.1109/APEIE59731.2023.10347807

Fast Algorithm for Dynamic Range Expansion of Images in Optoelectronic Measurement Systems

Vladimir I. Guzhov
Faculty of Automation and Computer Engineering
Novosibirsk State Technical University
Novosibirsk, Russian Federation
vigguzhov@gmail.com

Sergey P. Ilinykh
Faculty of Automation and Computer Engineering
Novosibirsk State Technical University
Novosibirsk, Russian Federation
isp51@yandex.ru

Vladimir K. Shperling
Faculty of Automation and Computer Engineering
Novosibirsk State Technical University
Novosibirsk, Russian Federation
vladimir-shperling@yandex.ru

Dmitry S. Khaidukov
Faculty of Automation and Computer Engineering
Novosibirsk State Technical University
Novosibirsk, Russian Federation
dmitriyhaydukov@gmail.com

***Abstract*—The paper proposes a new fast method for increasing the dynamic range of brightness of images projected onto an object and registered by an optoelectronic system. The influence of photon noise on the accuracy of brightness values determination is analyzed. An algorithm realizing the increase of the dynamic range of brightness of images registered by the optoelectronic system is proposed. For this purpose, a three-color RGB image is projected onto an object. Each channel contains encoded information about the brightness field in one of the selected modules of the residual class system. An experimental validation of the proposed algorithm is carried out. The dynamic range extension up to 20 binary digits of digital image digitization is achieved. The speed of data processing was increased several times due to combining several test images into one and using a cascade scheme of their processing.**

Keywords—dynamic range, number of quantization levels, quantization error, photon noise, optoelectronic measuring system, residual class system, digital image brightness

I. INTRODUCTION

Optoelectronic measuring systems have found wide application in modern science and technology [1-4]. Digital matrices for recording the intensity of optical images currently have a digitization capacity of about 8-14 bits. The error of phase measurements is limited, on the one hand, by the small dynamic range of the recorded optical images, and on the other hand, by the level of photon noise (oscillations of the light flux) that depends on it [5-6]. It was shown in [7] that the photon noise level is equal to the square root of the average intensity of the optical image. Thus, expanding the dynamic range leads to an increase in the level of photon noise. This leads to a decrease in the effective number of quantization levels of optical images by 1-2 or more binary digits. In [8], a method for increasing the dynamic range by recording several images with different optical shutter exposure times was considered. However, to significantly expand the dynamic range, this method requires recording a large number of images, which reduces the measurement speed. The purpose of the work is to modify the method of expanding the dynamic range when registering optical images from two or more images with a lower dynamic range, based on modular arithmetic proposed by the authors in [9].

II. THEORY

Let us consider the influence of photon noise depending on the image bit size (Fig. 1). The photon noise level for 8, 16, 24 and 32-bit images was calculated by the following formula [7]

$$\Delta b = \sqrt{B}\ , \tag{1}$$

here - Δb is the photon noise level, and. B is the brightness of the digital image.

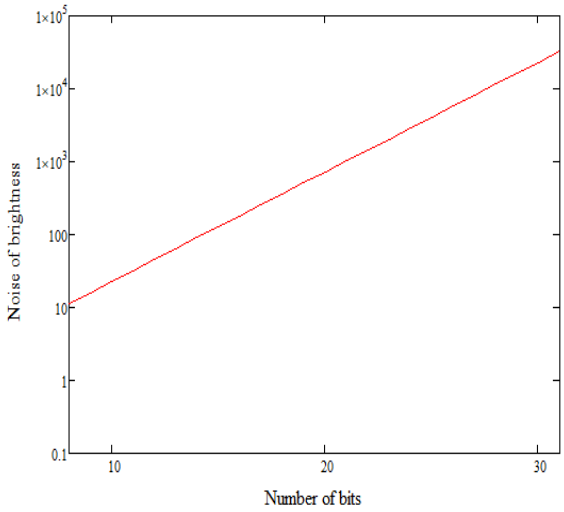

Fig. 1. Dependence of the photon noise level on the number of digits of a digital image.

It follows from Fig. 1 that the expansion of the dynamic range of image brightness leads to an increase in photon noise.

The presence of photon noise leads to inaccuracy in determining the true brightness value. Fig. 2 shows the dependence of the true brightness value determination error on the number of digits of the digital image. It follows from Fig. 1 that the expansion of the dynamic range of image brightness leads to an increase in photon noise. In the figures, the vertical axes are shown in logarithmic scale.

The presence of photon noise leads to inaccuracy in determining the true brightness value. Fig. 2 shows the dependence of the true brightness value determination error on the number of digits of the digital image.

It is shown in [9] that extending the dynamic range of brightness requires solving a system of comparisons in residual classes [10]

$$\begin{cases} B = b_1 + \left(2^{M_1} - 1\right) n_1 \\ B = b_2 + \left(2^{M_2} - 1\right) n_2 \end{cases}, \quad (2)$$

here B - brightness of the digital image with a large number of digits, b - brightness of the digital image with a small number of digits M, a n - $\max(B) \Big/ \left(2^M - 1\right)$ multiplier defined as an integer from division.

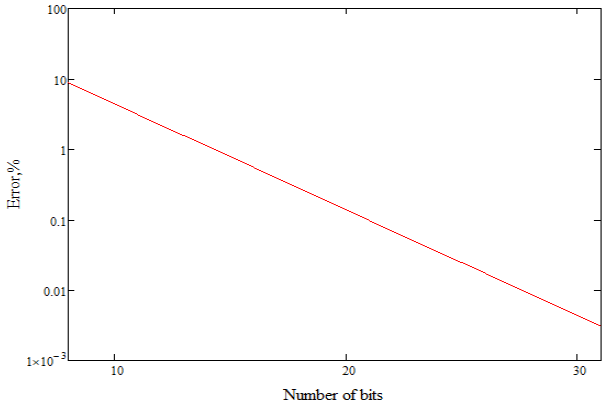

Fig. 2. Dependence of the brightness detection error on the number of digits of the digital image.

Note that the maximum brightness level depends on the number of low-bit-rate digital images

$$\max(B) = \prod_i M_i - 1 \cdot \quad (3)$$

So for two 8-bit images the maximum brightness at $M_1 = 251$ and $M_1 = 233$ the maximum brightness is $\max(B) = 48740$. This corresponds to 14-bit digitization of the image for $\max(B) = 16296073$ these values will be, and the number of digits will reach 24 ($\max(B) = 16296073$). Mostly 8-bit digital cameras are used for digital image registration because of their relatively low cost. Therefore, in order to achieve large values of dynamic range extension, the number of registered images should be increased. However, this leads to an increase in measurement time. Here we consider the case when one combined three-color image is registered with 8-bit digitization. This approach is often used in projection image synthesis [11]. In this case, separating the color channels Red, Green and Blue we obtain: $M_1 = 211$, $M_2 = 233$ and $M_3 = 251$. Then the maximum brightness is $\max(B) = 12233990$, and the number of digits reaches 24. Fig. 3 shows images of color channels and the resulting three-color image for linearly increasing brightness from zero to maximum brightness $\max(B) = 16296073$.

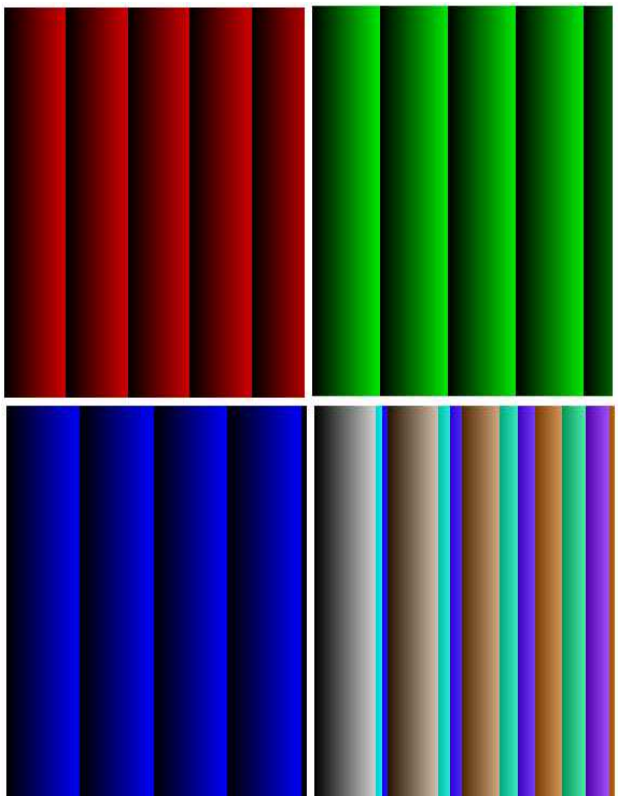

Fig. 3. Color channels and the resulting three-color image.

Let's note some peculiarities of using the combined three-color image [10] to expand the dynamic range of brightness of the digital image. For better use of the dynamic range for 8-bit digitization the amplitudes of each channel are in the range 0-255 in this case for correct solution of the system of equations (2) the image registered by the camera after channel separation should be numbered in accordance with the modules of the system of comparisons

$$\begin{aligned} \delta_1 &= \frac{M_1}{255} b_1 \\ \delta_2 &= \frac{M_2}{255} b_2 \cdot \\ \delta_3 &= \frac{M_3}{255} b_3 \end{aligned} \quad (4)$$

Then the system of equations (2) will take the following form

$$\begin{cases} B = \delta_1 + \left(2^{M_1} - 1\right) n_1 \\ B = \delta_2 + \left(2^{M_2} - 1\right) n_2 \cdot \\ B = \delta_3 + \left(2^{M_3} - 1\right) n_3 \end{cases} \quad (5)$$

Fig. 4 shows the graphical method of solving the system of equations (5). As can be seen from Fig. 4, the vertical section passing through the points δ_1 , δ_2 and δ_3 will correspond to a single point, which will be the solution of the system (5).

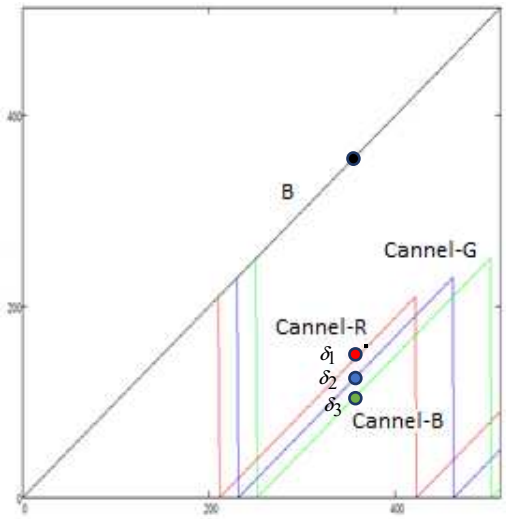

Fig. 4. Graphical method of solving the system of equations (5).

All possible solutions of the system (5) are conveniently represented as a set of tables (Fig.5).

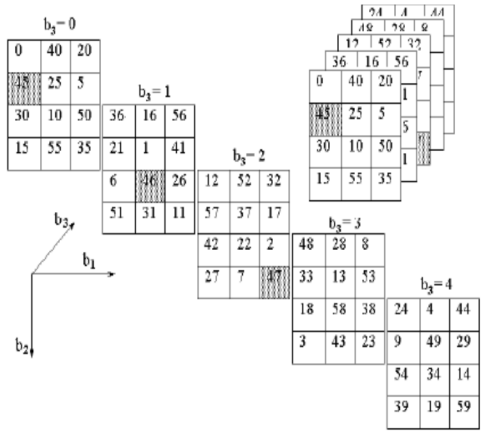

Fig. 5. Table of solutions of the system of equations (5).

In fact, the solution of the system (5) is an algorithm for converting integers from the modular number system to the positional number system. To perform this operation, it is enough to select a cell from the pre-built three-dimensional table (Fig. 5), which is constructed by calculating the indices δ_1, δ_2 and δ_3 the sequentially increasing linear function B.

Below we present an algorithm that implements this approach:

Step 1) set the values of the linear function in the partition $B \in [0,\ldots,M_1M_2M_3-1]$.

Step 2) calculate the table indices δ_i as a deduction from the modulo M_i value of the function B

$$\delta_i = B \bmod (M_i). \quad (6)$$

Step 3. form a table of values B corresponding to the indices δ_i.

$$T(\delta_1,\delta_2,\delta_3) = B_i. \quad (7)$$

The required amount of memory for storing the table is defined as

$$N_1 \le M_1 \times M_2 \times M_3 \times \text{int}\left[\log_2(M_1 \times M_2 \times M_3)\right]. \quad (8)$$

For example, for the selected modules of the system (5) we obtain $N_1 \approx 3 \cdot 10^8$ bit. It is possible to reduce the amount of required memory at the expense of some decrease in the speed of the algorithm. Note that for positioning in the table $T(\delta_1,\delta_2,\delta_3)$ it is enough to save only the first rows and columns for each dimension of the table $T(\delta_1,\delta_2,\delta_3)$

$$N_2 \le (M_1+M_2+M_3) \times \text{int}\left[\log_2(M_1 \times M_2 \times M_3)\right]. \quad (9)$$

In this case, the gain amounted to $\eta = N_1/N_2 = 1{,}76 \cdot 10^4$ times.

In the case of a multi-module comparison system, for example, only two tables of size $T_1(M_1 \times M_2)$ and $T_2((M_1 \times M_2) \times M_3)$ respectively can be generated for three modules.

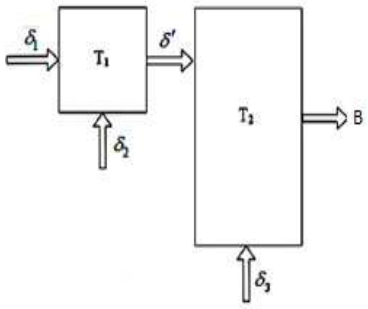

Fig. 6. Cascade schame of construction of the three-module algorithm.

Below are TABLE I and TABLE II corresponding to the tables T_1 and T_2 shown in Fig. 6 for the residual class system modules 3, 5 and 7 generated by the system of equations (5). Tables have dimensions $T_1(3\times5)$ and $T_2((3\times5=15)\times7)$ respectively Here, the color highlights the ways to obtain a solution for $B=53$. For the brigthness $B=53$ $\delta_1 = 53 \bmod (3) = 2$, and $\delta_2 = 53 \bmod (5) = 3$, then the deduction $\delta' = 53 \bmod (15) = 8$ and deduction $\delta_1 = 53 \bmod (7) = 4$. The order of table construction is given in more detail in the work of the authors [9].

TABLE I. DEDUCTIONS FOR MODULES 3 AND 5

δ_1/δ_2	0	1	2	3	4
0	0	6	12	3	9
1	10	1	7	13	4
2	5	11	2	8	14

TABLE II. DEDUCTIONS FOR MODULES 5 AND 15

δ'/δ_2	0	1	2	3	4	5	6	7	8	9	10	11	12	13	14
0	0	91	77	63	49	35	21	7	98	84	70	56	42	28	14
1	15	1	92	78	64	50	36	22	8	99	85	71	57	43	29
2	30	16	2	93	78	64	51	37	23	9	100	86	72	58	44
3	45	31	17	3	94	80	66	52	38	24	10	101	87	73	59
4	60	46	32	18	4	95	81	67	53	39	25	11	102	88	74
5	75	61	47	33	19	5	96	82	68	54	40	26	12	103	89
6	90	76	62	48	34	20	6	97	83	69	55	41	27	13	104

III. EXPEREMENTAL RESULTS

To test the performance of the proposed algorithm, a three-color image of 4000x3000 pixels was synthesized using rule (4) (see Fig. 3). The image was projected onto a 1m×1m white screen by a Sony VPL - VW260ES projector from a distance of 1.5m. The optical axis of the projector was oriented perpendicular to the screen plane. The image compressed on the object was registered by a CANON EOS 600 camera at the same distance at an angle to the screen plane. Then a digital image with a large number of quantization equations was reconstructed by algorithm (6) - (9) (see Fig. 7).

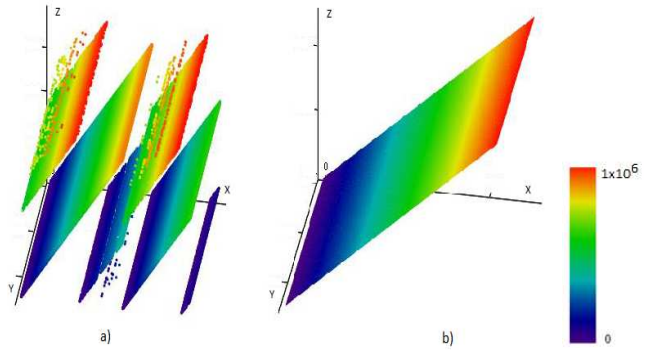

Fig. 7. Results of cyr image synthesis; (a) - without correction, (b) after correction.

It follows from Fig. 7,a that the reconstructed image contains a large number of gross errors, which are caused by incorrect definition of deductions, since the photon noise level is greater than the difference between the elements of the first row and the first column of the deduction table (see Tables I and II). It is possible to increase the robustness of the algorithm to noise by limiting the maximum brightness range of the reconstructed image. In this case the diagonals are thinned and the difference between adjacent table elements increases. The greater the value of the limitation, the greater the distance between diagonals. Fig.7, b Shows the results of image restoration after limiting the maximum range to a value equal to . The obtained maximum range after correction is equal to 1.6×106, which corresponds to 20-bit quantization level.

IV. CONCLUSIONS

An algorithm realizing this principle is proposed. The product of the modules determines the dynamic range of the represented values of the brightness field of the image. The influence of photon noise on the accuracy of determining the brightness values is analyzed. It is shown that increasing the dynamic range leads to an increase in the level of photon noise The cascade scheme of construction of the three-module algorithm is proposed, which allows to reduce the level of photon noise. Experimental verification of the proposed algorithm is carried out. It is established. That the level of photon noise of 8-bit quantization does not allow to use the whole range of brightness variation of the synthesized image. Correction of the algorithm parameters was performed. The maximum dynamic range of the brightness of the three-color image after correction was 1.6×10^6, which corresponds to the 20-bit quantization level. The speed of data processing is increased several times due to combining several test images into one image and using a cascade scheme of their processing.

REFERENCES

[1] J Jensen, J. Hannemose, M. Bærentzen, A. Wilm, J. Frisvad, J. Dahl, "Surface Reconstruction from Structured Light Images Using Differentiable Rendering," Sensors, February 2021, vol. 21(4), pp. 1068. doi:10.3390/s21041068.

[2] A. Gauthier, S. Verbanck, M. Estenne, C. Segebarth, P. Macklem, M. Paiva "Three-dimensional reconstruction of In Vivo human lumbar spine from biplanar radiographs," Comput. Med. Imaging Graph. 2022, 96, 102011, doi: 10.1152/jappl.1994.76.2.495

[3] S. Zhang, "High-speed 3D shape measurement with structured light methods: A review," Opt. Lasers Eng. 2018, 106, pp. 119–131, doi:10.1016/j.optlaseng.2018.02.017.

[4] H. Nguyen, K. Ly, T. Nguyen, Y. Wang, Z. Wang, "MIMONet: Structured-light 3D shape reconstruction by a multi-input multi-output network," Appl. Opt. 2021, vol. 60, pp. 5134–5144, doi:10.1364/ao.426189.

[5] Li, Dongxue & Xu, Fang & Wang, Hongyu & Wu, Chengdong & Zou, Fengshan & Song, Jilai. "Lasers structured light with phase-shifting for dense depth perception,". Results in Physics, 14. 102433, doi:10.1016/j.rinp.2019.102433.

[6] Tran, V.; Lin, H.Y. "A Structured Light RGB-D Camera System for Accurate," Depth Measurement. Int. J. Opt. 2018, vol. 2018, doi:10.1155/2018/8659847.

[7] I.N. Pustynskiy, E.V. Zaitseva "To calculation of image illumination and number of signal electrons in a TV sensor on a CCD matrix [K raschetu osveshhennosti izobrazheniya i kolichestva signal`ny`x e`lektronov v televizionnom datchike na PZS-matrice]," (in Russian), Papers of Tomsk State University of Control Systems and Radioelectronics, 2009, № 2, pp. 5-10.

[8] Kiran, Bagadi Ravi, Kumari, Vatsavayi Valli and Raju, "Model for High Dynamic Range Imaging System Using Hybrid Feature Based Exposure Fusion [Model` dlya sistemy` vizualizacii s vy`sokim dinamicheskim diapazonom, ispol`zuyushhej gibridnoe ob``edinenie e`kspozicii na osnove funkcij]," (in Russian), Journal of Intelligent Systems, vol. 30, no. 1, 2021, pp. 346-360, doi:10.1515/jisys-2018-0412.

[9] V.I. Guzhov, S.P. Ilinykh, D.S Khaidukov, "Method for increasing the dynamic range of digital images based on modular arithmetic," Journal of Physics: Conference Series 1661(1),012040. – 2020, pp. 1-6, doi: 10.1088/1742-6596/1661/1/012040.

[10] V.I. Guzhov "Methods of measuring 3D profile of objects. Phase methods [Metody` izmereniya trexmernogo profilya ob``ektov. Fazovy`e metody`], " (in Russian), Novosibirsk: Izd-vo NSTU, 2016, p. 83.

[11] Niu Z, Xu X, Zhang X, Wang W, Zhu Y, Ye J, Xu M, Jiang X. "Efficient phase retrieval of two-directional phase-shifting fringe patterns using geometric constraints of deflectometry," Opt Express, 2019 Mar 18, vol.27(6), pp.8195-8207, doi: 10.1364/OE.27.008195.